© 2018. Published by The Company of Biologists Ltd | Journal of Experimental Biology (2018) 221, jeb179226. doi:10.1242/jeb.179226

RESEARCH ARTICLE

Expression of calcium channel transcripts in the zebrafish heart: dominance of T-type channels

Jaakko Haverinen[1,*], Minna Hassinen[1], Surjya Narayan Dash[1,2] and Matti Vornanen[1]

ABSTRACT

Calcium channels are necessary for cardiac excitation–contraction (E–C) coupling, but Ca^{2+} channel composition of fish hearts is still largely unknown. To this end, we determined transcript expression of Ca^{2+} channels in the heart of zebrafish (*Danio rerio*), a popular model species. Altogether, 18 Ca^{2+} channel α-subunit genes were expressed in both atrium and ventricle. Transcripts for 7 L-type ($Ca_v1.1a$, $Ca_v1.1b$, $Ca_v1.2$, $Ca_v1.3a$, $Ca_v1.3b$, $Ca_v1.4a$, $Ca_v1.4b$), 5 T-type ($Ca_v3.1$, $Ca_v3.2a$, $Ca_v3.2b$, $Ca_v3.3a$, $Ca_v3.3b$) and 6 P/Q-, N- and R-type ($Ca_v2.1a$, $Ca_v2.1b$, $Ca_v2.2a$, $Ca_v2.2b$, $Ca_v2.3a$, $Ca_v2.3b$) Ca^{2+} channels were expressed. In the ventricle, T-type channels formed 54.9%, L-type channels 41.1% and P/Q-, N- and R-type channels 4.0% of the Ca^{2+} channel transcripts. In the atrium, the relative expression of T-type and L-type Ca^{2+} channel transcripts was 64.1% and 33.8%, respectively (others accounted for 2.1%). Thus, at the transcript level, T-type Ca^{2+} channels are prevalent in zebrafish atrium and ventricle. At the functional level, peak densities of ventricular T-type (I_{CaT}) and L-type (I_{CaL}) Ca^{2+} current were 6.3±0.8 and 7.7±0.8 pA pF^{-1}, respectively. I_{CaT} mediated a sizeable sarcolemmal Ca^{2+} influx into ventricular myocytes: the increment in total cellular Ca^{2+} content via I_{CaT} was 41.2±7.3 µmol l^{-1}, which was 31.7% of the combined Ca^{2+} influx (129 µmol l^{-1}) via I_{CaT} and I_{CaL} (88.5±20.5 µmol l^{-1}). The diversity of expressed Ca^{2+} channel genes in zebrafish heart is high, but dominated by the members of the T-type subfamily. The large ventricular I_{CaT} is likely to play a significant role in E–C coupling.

KEY WORDS: *Danio rerio*, E–C coupling, Cardiac myocytes, T-type Ca^{2+} current, Zebrafish heart

INTRODUCTION

Voltage-gated Ca^{2+} channels enable Ca^{2+} influx into cells and mediate a wide variety of physiological responses including muscle contraction, hormone secretion, neuronal transmission, gene expression and cell division (McDonald et al., 1994; Hofmann et al., 2014). In the sarcolemma of cardiac myocytes, two major types of Ca^{2+} channel are usually present: L-type (long-lasting, high-threshold) Ca^{2+} channels of the subfamily Ca_v1 and T-type (transient, low-threshold) Ca^{2+} channels of the subfamily Ca_v3 (Ertel et al., 2000; Catterall et al., 2005).

In the mammalian heart, L-type Ca^{2+} channels are abundantly expressed in atrial and ventricular myocytes, sinoatrial pacemaker cells and atrioventricular nodal cells (Hagiwara et al., 1988; Zamponi et al., 2015; Mesirca et al., 2015). L-type Ca^{2+} current (I_{CaL}) is a critical component in excitation–contraction (E–C) coupling of atrial and ventricular myocytes by inducing Ca^{2+} release (Ca^{2+}-induced Ca^{2+} release, CICR) from the sarcoplasmic reticulum (SR) (Fabiato, 1983; Bers, 2002). In sinoatrial myocytes, I_{CaL} generates the upstroke of pacemaker action potential (AP) (Irisawa et al., 1993). In cardiac myocytes of fetal and neonatal mammals and ectothermic vertebrates, I_{CaL} directly contributes to the cytosolic Ca^{2+} transient, as CICR is less powerful in these cells (Fabiato and Fabiato, 1978; Morad et al., 1981; Vornanen, 1996; Vornanen et al., 2002).

The distribution of T-type Ca^{2+} channels and current (I_{CaT}) is more limited in the adult mammalian heart. T-type Ca^{2+} channels are strongly expressed in sinoatrial and atrioventricular nodes, weakly expressed in atrial myocytes and are usually not present in healthy ventricular myocytes (Perez-Reyes, 2003; Ono and Iijima, 2010). It should be noted, however, that a small I_{CaT} is present in guinea-pig and dog ventricular myocytes (Nilius et al., 1985; Mitra and Morad, 1986; Balke et al., 1992; Wang and Cohen, 2003). I_{CaT} has a significant role in cardiac pacemaking by contributing to the diastolic depolarization of pacemaker AP, while its significance in E–C coupling of atrial and ventricular myocytes is incompletely resolved (Zhou and January, 1998; Kitchens et al., 2003; Jaleel et al., 2008; Ono and Iijima, 2010; Mesirca et al., 2015). I_{CaT} is upregulated in diseased mammalian heart, including genetic hypertension, cardiac hypertrophy and atherosclerosis (Takebayashi et al., 2006; Chiang et al., 2009).

I_{CaL} has been recorded in atrial and ventricular myocytes of several fish species including the zebrafish (*Danio rerio*) (Maylie and Morad, 1995; Vornanen, 1997, 1998; Hove-Madsen and Tort, 1998; Vornanen et al., 2002; Shiels et al., 2006; Brette et al., 2008; Zhang et al., 2011; Galli et al., 2011; Haworth et al., 2014; Haverinen et al., 2014). I_{CaT} has been shown to be present in atrial and ventricular myocytes of the dogfish (*Squalus acanthias*) and zebrafish hearts, and in atrial myocytes of the Siberian sturgeon (*Acipenser baerii*) heart (Maylie and Morad, 1995; Warren et al., 2001; Nemtsas et al., 2010; Haworth et al., 2014). In contrast to the rich data on the mammalian cardiac Ca^{2+} channels, very little is known about Ca^{2+} channels of the fish heart, even though sarcolemmal Ca^{2+} channels play a central role in cardiac E–C coupling of fish (Vornanen et al., 2002; Zhang et al., 2011). There is also little knowledge about the molecular and genetic background of cardiac Ca^{2+} channels in zebrafish (Rottbauer et al., 2001), which is somewhat surprising considering that this species is a popular model for cardiovascular drug screening and human cardiac diseases (Bakkers, 2011; MacRae and Peterson, 2015). To be a useful model for the human heart, it is crucial to know the molecular basis of Ca^{2+} currents in the zebrafish heart, as Ca^{2+} channels are important therapeutic targets for the treatment of cardiovascular diseases (Belardetti and Zamponi, 2012). To this end, we measured Ca^{2+} channel transcript expression in the zebrafish heart. In addition, Ca^{2+} influx via I_{CaT} and I_{CaL} into zebrafish ventricular myocytes was

[1]Department of Environmental and Biological Sciences, University of Eastern Finland, PO Box 111, 80101 Joensuu, Finland. [2]Neuroscience Center and Department of Anatomy, Faculty of Medicine, University of Helsinki, PO Box 63, 00014 Helsinki, Finland.

*Author for correspondence (jaakko.haverinen@uef.fi)

J.H., 0000-0002-2300-6849

Received 12 February 2018; Accepted 6 April 2018

determined using the whole-cell patch-clamp method. Because I_{CaL} is generally regarded as the most important cardiac Ca^{2+} current, our working hypothesis was that different L-type Ca^{2+} channels form the dominant Ca^{2+} channel subfamily in the zebrafish atrium and ventricle.

MATERIALS AND METHODS

Zebrafish

The wild-type Turku zebrafish line (kindly donated by Prof. Pertti Panula, University of Helsinki) was raised and maintained at the animal facilities of UEF (University of Eastern Finland, Joensuu) according to the established principles (Westerfield, 2007). The rearing temperature of the fish was 28°C. The experiments conform to the European Convention for the Protection of Vertebrate Animals used for Experimental and other Scientific Purposes (Council of Europe No. 123, Strasbourg 1985) and were authorized by the national animal experimental board in Finland (permission ESAVI/2832/04.10.07/2015).

Total RNA isolation and quantification of gene expression

Fish were killed by immersing them in ice water and the heart was excised. Total RNA was isolated from three atrial and ventricular samples (see 'Patch-clamp analysis of I_{CaT} and I_{CaL}', below) (each containing cardiac tissue of eight adult zebrafish, 1.5 years old) using TriReagent (Thermo Scientific, Waltham, MA, USA). RNA was DNase treated with RNase-free DNaseI (Thermo Scientific) and reverse-transcribed with random hexamer and oligo(dT) primers and Maxima RNase H-reverse transcriptase (Thermo Scientific) following the manufacturer's protocols. In order to design gene-specific primers for qPCR, a and b isoforms of each *cacna* (*α1*) gene were aligned and primers were designed to non-homologous regions. Moreover, all 18 *α1* genes were aligned using Clustal Omega (https://www.ebi.ac.uk/Tools/msa/clustalo/) and the specificity of primers was checked. Finally, PrimerBlast (https://www.ncbi.nlm.nih.gov/tools/primer-blast/) was used to validate the targets of each primer pair. qPCR was performed using Maxima SYBR Green qPCR Master Mix (Thermo Scientific) in an Aria MX Real-Time PCR machine (Agilent Technologies, Santa Clara, CA, USA). Accession numbers of the genes and primers used in this study are listed in Table 1. The thermal conditions were as follows: enzyme activation at 95°C for 10 min followed by 40 cycles at 95°C for 10 s, 58°C for 20 s and 72°C for 30 s, and final extension at 72°C for 3 min. After the qPCR reaction, the specificity of amplification was checked by melting curve analysis (from 65 to 95°C) and by

Table 1. Primers used for qPCR

Protein	Gene	Accession number	Primer sequence	Amplicon length (bp)
$Ca_v1.1a$	*α1Sa*	NM_001146150	TCTATAGGCGTGCTGGAGGT GCTATCTGCGAGCTGTAGGG	113
$Ca_v1.1b$	*α1Sb*	NM_214726	GTTGGCTGAAGACCCACAGT GCCCATTGACAATACCCTGA	110
$Ca_v1.2$	*α1C*	XM_009300335	ACGGAGTCACTCTCCGACAC AGAGAGGGCACAGGCTGATA	105
$Ca_v1.3a$	*α1Da*	NM_203484	ACTGGGCCACAGAGACTACG TTCATCTGCAAGGTCCTCC	106
$Ca_v1.3b$	*α1Db*	ENSDARG00000101589	CGCAAACAGAGTCAGGATCA GAGTCGTGATTGGCTGGATT	105
$Ca_v1.4a$	*α1Fa*	XM_021478483	AGCAGCCTCGAGCATACACT CCCAAGCCTTCAGAAATCAG	115
$Ca_v1.4b$	*α1Fb*	NM_001324496	ATTGACCAACTGCCCAAGAG GCTCTCCAGGGTACTCACCA	115
$Ca_v2.1a$	*α1Aa*	ENSDARG00000037905	TGCTACCCAGCCACATGATA TGGTAGAGGAAGGGTTGGTG	113
$Ca_v2.1b$	*α1Ab*	ENSDARG00000006923	CTGCGTGGACCAGATCTACA GGCATTGAGTGAGGGGTAAA	105
$Ca_v2.2a$	*α1Ba*	ENSDARG00000021735	CAATGCTGAGATGCAGAGGA CTGTGGTGCAAAAGTGGATG	106
$Ca_v2.2b$	*α1Bb*	ENSDARG00000079295	TGCTTCCTCTCACACACCTG AAAGAAGTGGGTGTGGCATC	106
$Ca_v2.3a$	*α1Ea*	ENSDARG00000062346	GCAGCTCGAGGAACAGAAAC CCTGCACTGTGAGTCAGGAA	114
$Ca_v2.3b$	*α1Eb*	ENSDARG00000095614	ACTACGACGCCTCACAGGTT TGGGACACTGCAGCTTTGTA	115
$Ca_v3.1$	*α1G*	ENSDARG00000089913	CTTGGCACCGGTTGTGTTTT CATACTGGCCCTCTCGAACC	100
$Ca_v3.2a$	*α1Ha*	ENSDARG00000060496	TCCATCGAGCATTTCAATCA GCCACGAGTTTAAGCAGAGC	107
$Ca_v3.2b$	*α1Hb*	ENSDARG00000099708	TGTTTCGGGGTCTGTGAGTG ACTCTGCGTTTCGGGACATT	120
$Ca_v3.3a$	*α1Ia*	ENSDARG00000070522	TGTTCACGAAAGAGCCACAG TGGCTTGTACTTTCCCCATC	103
$Ca_v3.3b$	*α1Ib*	ENSDARG00000096307	TTCCCCATCAGAAACCTCAC TGAGATTCTGTTTGCGCA	107
β-actin	*actb1*	NM_131031	CTTCCAGCAGATGTGGATCA GCCATTTAAGGTGGCAACA	102
DnaJA2	*dnaja2*	NM_213493	CTATGGGGAACAGGGTCTGC GTCCACCCATGAAACCAAAC	104

Primers are in the 5′–3′ orientation.

Journal of Experimental Biology (2018) 221, jeb179226. doi:10.1242/jeb.179226

running the qPCR products on an agarose gel. Data were normalized to the geometric mean of *dnaja2* (DnaJ homologue subfamily A member 2) and *actb1* (β-actin) mRNA expression levels.

Patch-clamp analysis of I_{CaT} and I_{CaL}

Electrophysiological experiments were conducted on enzymatically isolated ventricular myocytes of adult zebrafish (1.5 years old, 0.68±0.03 g). Fish were stunned with a quick blow to the head, the spine was cut and the heart was excised. The yield of atrial myocytes was low and therefore extensive characterization of atrial electrophysiology was not possible. The myocyte isolation procedure was essentially similar to our original isolation method for fish hearts (Vornanen, 1997), but scaled down to the size of small zebrafish hearts. For retrograde perfusion of the heart, a small cannula (34 gauge, TE734025, Adhesive Dispensing Ltd, Milton Keynes, Bucks, UK) was inserted via the bulbus arteriosus into the ventricle and the bulbus was secured with a fine thread around the cannula. The heart was perfused first with Ca^{2+}-free solution for 5 min and then with the same solution but with added hydrolytic enzymes [Collagenase Sigma IA, Trypsin type VI (Serva, Heidelberg, Germany) together with fatty acid-free serum albumen] for 15–20 min. Myocytes were stored at 5°C and used on the same day they were isolated. The composition of the Ca^{2+}-free solution was (in mmol l^{-1}): 100 NaCl, 10 KCl, 1.2 KH_2PO_4, 4 $MgSO_4$, 50 taurine, 20 glucose and 10 Hepes, with pH adjusted to 6.9 with KOH at 20°C.

An Axopatch 1D amplifier (Axon Instruments, Saratoga, CA, USA) with a CV-4 1/100 head-stage was used for whole-cell patch-clamp experiments. The external solution used for I_{CaT} and I_{CaL} recordings contained (in mmol l^{-1}): 20 CsCl, 120 tetraethylammonium chloride, 1 $MgCl_2$, 2 $CaCl_2$, 10 glucose and 10 Hepes (pH adjusted to 7.7 with CsOH). The solution was Na^+ free and included 0.5 µmol l^{-1} tetrodotoxin (Tocris Cookson, Bristol, UK) to prevent Na^+ current (I_{Na}). As Cs^+ can flow through Erg K^+ channels, 2 µmol l^{-1} E-4031 (Tocris Cookson) was included in the external saline solution to prevent the rapid component of the delayed rectifier K^+ current (I_{Kr}). Temperature was regulated at 28°C by using a Peltier device (HCC-100A, Dagan, MN, USA). The pipette solution contained (in mmol l^{-1}) 130 CsCl, 15 tetraethylammonium chloride, 5 MgATP, 1 $MgCl_2$, 5 oxaloacetate, 10 Hepes and 5 EGTA (pH adjusted to 7.2 at 20°C with CsOH) (all chemicals from Sigma, St Louis, MO, USA), giving a mean (±s.e.m.) resistance of 2.5±0.03 MΩ.

After gaining a giga-ohm seal and access to the cell, current transients due to series resistance (6.17±0.22 MΩ) and pipette capacitance (8.20±0.10 pF) were cancelled out, and the capacitive size of ventricular myocytes (27.77±1.11 F, n=62) was determined. The total I_{Ca}, including both I_{CaT} and I_{CaL}, was elicited by 300 ms square wave pulses from the holding potential (V_h) of −90 mV with 10 mV increments to cover a voltage range from −80 to +50 mV. I_{CaL} was elicited from a V_h of −50 mV to voltages ranging from −40 to +50 mV. I_{CaT} was obtained as the difference current from these two protocols.

Charge transfer through Ca^{2+} channels was determined by integrating the inactivating portion of the Ca^{2+} current for 300 ms voltage pulses from −90 mV to −30 mV for I_{CaT} and from −50 mV to 0 mV for I_{CaL}. The change in total intracellular cellular Ca^{2+} concentration ($[Ca^{2+}]_i$) due to Ca^{2+} influx via T-type and L-type Ca^{2+} channels was calculated from the measured cell capacitance and the experimentally determined surface-to-volume ratio of the cells (1.15): as described earlier in detail (Vornanen, 1997). $[Ca^{2+}]_i$ was expressed for the non-mitochondrial cell volume assuming a non-mitochondrial volume fraction of 0.55.

Statistics

Statistics were performed using SPSS version 21.0. Statistically significant differences between sarcolemmal Ca^{2+} influxes by I_{CaT} versus I_{CaL} were detected through Mann–Whitney U non-parametric test for two independent samples, after checking the normality of distribution and carrying out necessary transformation of the data. Differences between mean transcript expression values of the five Ca^{2+} channel types and concentration-dependent I_{CaT} inactivation by Ni^{2+} were compared using one-way ANOVA followed by Tukey's *post hoc* test. Paired comparisons between transcripts of Ca^{2+} channel genes and T- and L-type Ca^{2+} current were done by two-tailed Student's t-test. The significance threshold was P<0.05.

RESULTS

Expression of Ca^{2+} channel transcripts

We performed qPCR to investigate the mRNA expression of T-type ($Ca_v3.1$, $Ca_v3.2a$, $Ca_v3.2b$, $Ca_v3.3a$ and $Ca_v3.3b$), L-type ($Ca_v1.1a$, $Ca_v1.1b$, $Ca_v1.2$, $Ca_v1.3a$, $Ca_v1.3b$, $Ca_v1.4a$ and $Ca_v1.4b$), P/Q-type ($Ca_v2.1a$ and $Ca_v2.1b$), N-type ($Ca_v2.2a$ and $Ca_v2.2b$) and R-type ($Ca_v2.3a$ and $Ca_v2.3b$) Ca^{2+} channel α-subunit genes in the atrium and ventricle of 1.5 year old zebrafish. Interestingly, in the atrium, transcript expression of T-type Ca^{2+} channels (64.1±3.7% of all Ca_v transcripts) was significantly higher than that of L-type Ca^{2+} channels (33.8±3.4%; P<0.05) (Fig. 1). In the ventricle, T-type channel transcripts (54.9±4.4%) seemed to be more numerous than L-type channel transcripts (41.1 ±4.4%), but the difference was not statistically significant (P>0.05). Transcripts of P/Q-type channels constituted 1.7 ±0.3% and 4.0±0.5% of all Ca^{2+} channel transcripts in the atrium and ventricle, respectively (Fig. 1). N- and R-type Ca^{2+} channel transcripts were also present, but the expression levels were low in both cardiac chambers (less than 0.5% of all Ca_v transcripts).

At transcript level, the main T-type Ca^{2+} channel isoform in the zebrafish heart was *α1G* (encoding $Ca_v3.1$), representing

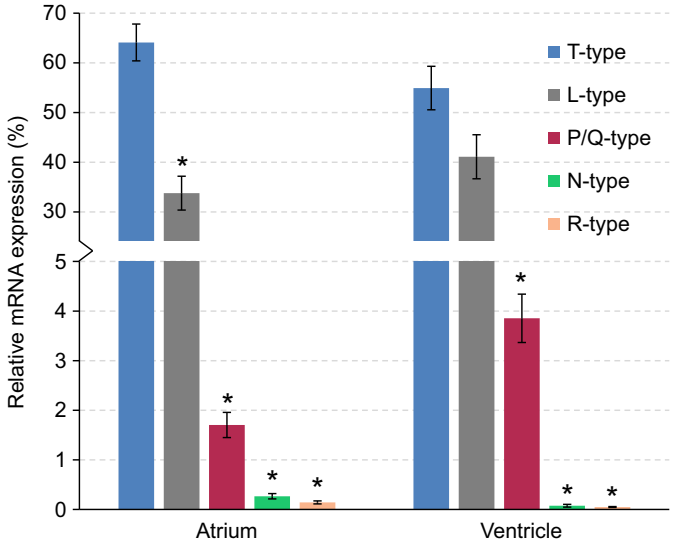

Fig. 1. Relative transcript expression of the five Ca^{2+} channel types in zebrafish atrium and ventricle. Data (means±s.e.m. of three samples, each representing pooled tissue from 8 fishes) are given as a percentage of all Ca^{2+} channel transcripts. An asterisk indicates a statistically significant difference (P<0.001) between T-type channels and the other Ca^{2+} channel types (pairwise comparisons between T-type channels and L-, P/Q-, N- and R-type channels using one-way ANOVA followed by Tukey's *post hoc* test).

Journal of Experimental Biology (2018) 221, jeb179226. doi:10.1242/jeb.179226

99.7±0.05% and 98.9±0.3% of T-type transcripts in the ventricle and atrium, respectively (Fig. 2). The dominant L-type Ca^{2+} channel isoform was $Ca_v1.2$ (encoded by the *α1C* gene), comprising 93.0±1.2% and 95.9±0.7% of all Ca_v1 transcripts in the ventricle and atrium, respectively (Fig. 2). Transcript expression of *α1G* was significantly ($P<0.05$) higher – in both the ventricle (54.8±4.4% of all Ca_v transcripts) and the atrium (63.4±3.9%) – than that of the dominant L-type Ca^{2+} channel, *α1C* (38.3±4.6% in the ventricle and 32.4±3.4% in the atrium) (Table 2). P/Q-type Ca^{2+} channel isoform $Ca_v2.1b$ (encoded by *α1Ab*) showed the third highest expression level, representing 3.8±0.5% and 1.6±0.3% of all Ca_v transcripts in the ventricle and atrium, respectively (Table 2). Collectively, these data show that *α1G* mRNA expression is dominant in both cardiac chambers of the adult zebrafish heart.

Density and voltage dependence of I_{CaT} and I_{CaL}

I_{CaL} was determined as the current elicited from a V_h of −50 mV. I_{CaT} was obtained by subtracting I_{CaL} from the current elicited from a V_h of −90 mV, where both channels are available for opening. Ventricular myocytes of the zebrafish heart had large I_{CaT} and I_{CaL} (Fig. 3). I_{CaT} had a peak current density of 6.3±0.8 pA pF^{-1} at −30 mV, whereas I_{CaL} peaked at 0 mV with a density of 7.7±0.8 pA pF^{-1} ($P>0.05$) (Fig. 3B). Densities of I_{CaT} and I_{CaL} varied markedly between individual ventricular myocytes (Fig. 3C). Typical densities for I_{CaL} were 4–6 pA pF^{-1}. The frequency distribution of I_{CaT} density was flatter than that of I_{CaL} without any typical density value.

Nickel sensitivity of I_{CaT}

T-type Ca^{2+} channels are blocked by Ni^{2+}. As $Ca_v3.1$ (*α1G*), $Ca_v3.2$ (*α1H*) and $Ca_v3.3$ (*α1I*) isoforms are differently sensitive to Ni^{2+} (Lee et al., 1999), inhibition of I_{CaT} by Ni^{2+} can be used to trace isoform composition of cardiac myocytes. To this end, Ni^{2+} sensitivity of I_{CaT} was examined by cumulative additions of $NiCl_2$ (0.3–1000 µmol l^{-1}) to the external saline solution. I_{CaT} was inhibited by Ni^{2+} in a concentration-dependent manner (Fig. 4A). Half-maximal inhibition (IC_{50}) occurred at 92.1±0.1 µmol l^{-1} Ni^{2+} (Fig. 4B). Ni^{2+} also slowed recovery from inactivation of I_{CaT} (Fig. 4B, inset).

Sarcolemmal Ca^{2+} entry via I_{CaT} and I_{CaL}

Sarcolemmal Ca^{2+} influx was obtained from the integrals of I_{CaT} and I_{CaL} at −50 and 0 mV, respectively (Fig. 5A). In ventricular myocytes, cytosolic Ca^{2+} increments via I_{CaT} and I_{CaL} were 41.2±7.3 and 88.5±20.5 µmol l^{-1} per non-mitochondrial cell volume, respectively (Fig. 5B). This means that I_{CaT} was responsible for 31.7% of the total Ca^{2+} influx via sarcolemmal Ca^{2+} channels.

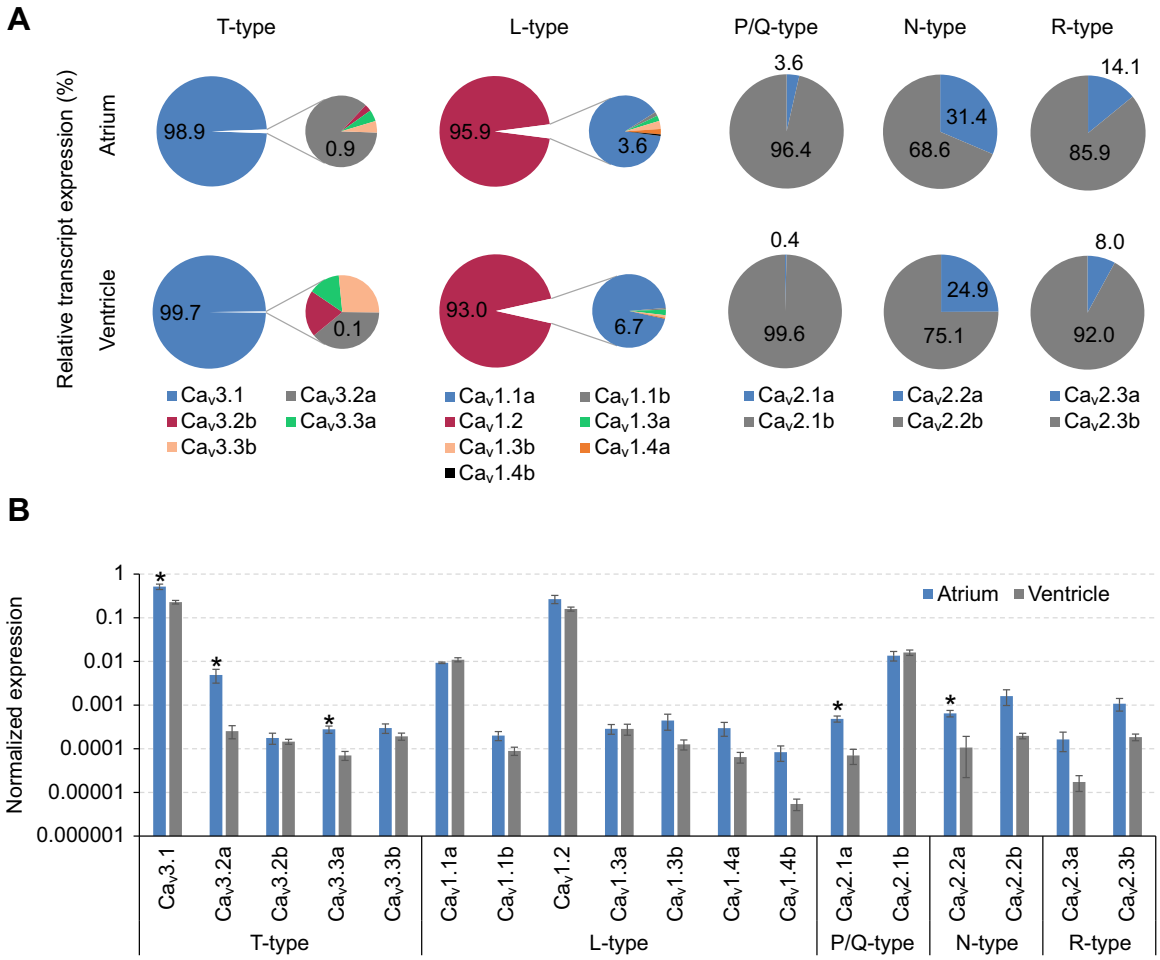

Fig. 2. Transcript expression of Ca^{2+} channel α-subunit genes in zebrafish atrium and ventricle. (A) Pie charts indicating the relative portions (%) of each Ca_v transcript from the total Ca^{2+} channel expression of each Ca^{2+} channel type. (B) Transcript expression of Ca_v genes in zebrafish atrium and ventricle normalized to the geometric mean expression of the reference genes *dnaJA2* and *β-actin*. The results are means±s.e.m. of three samples, each representing pooled tissue from 8 fishes. An asterisk indicates a statistically significant difference between atrium and ventricle ($P<0.05$, two-tailed Student's *t*-test).

Journal of Experimental Biology (2018) 221, jeb179226. doi:10.1242/jeb.179226

Table 2. Comparison of different calcium ion currents and channel genes (% of all transcripts) between zebrafish (present study) and human heart (Gaborit et al., 2007)

Ca^{2+} current	Channel	Zebrafish (atrium)	Zebrafish (ventricle)	Human (atrium)	Human (ventricle)
I_{CaT}	$Ca_v3.1$	63.44	54.76	3.02	0.14
	$Ca_v3.2a$	0.58	0.06	1.08	1.46
	$Ca_v3.2b$	0.02	0.03		
	$Ca_v3.3a$	0.04	0.02		
	$Ca_v3.3b$	0.04	0.05		
I_{CaL}	$Ca_v1.2$	32.43	38.33	94.77	98.36
	$Ca_v1.3a$	0.03	0.07	1.13	0.04
	$Ca_v1.3b$	0.05	0.03		
	$Ca_v1.4a$	0.03	0.02		
	$Ca_v1.4b$	0.01	0.001		
	$Ca_v1.1a$	1.20	2.63		
	$Ca_v1.1b$	0.02	0.02		
$I_{CaP/Q}$	$Ca_v2.1a$	0.06	0.02		
	$Ca_v2.1b$	1.64	3.84		
I_{CaN}	$Ca_v2.2a$	0.08	0.03		
	$Ca_v2.2b$	0.19	0.05		
I_{CaR}	$Ca_v2.3a$	0.02	0.004		
	$Ca_v2.3b$	0.12	0.04		

DISCUSSION

Ten Ca^{2+} channel α-subunit genes, divided into three subfamilies (Ca_v1–3), exist in vertebrate genomes (Catterall et al., 2005). Because of the whole-genome duplication in the early teleosts, fish genomes include a number of gene paralogues. Therefore, a higher diversity of Ca^{2+} channel genes is expected to exist in fish genomes (Jegla et al., 2009). Indeed, 21 α-subunit genes were found in the genome of fugu (*Fugu rubripes*) (Wong et al., 2006). In the current study, we provide a complete survey of Ca^{2+} channel α-subunit expression in the zebrafish heart. Transcript abundance of 18 Ca^{2+} channel α-subunit genes was quantified in the atrium and ventricle of the zebrafish heart. Several studies have shown that expression of ion channel proteins in the heart is predominantly determined at the level of transcription (Rosati and McKinnon, 2004; Marionneau et al., 2005; Gaborit et al., 2007; Chandler et al., 2009; Abd Allah et al., 2012). Therefore, we believe that the relative abundance of gene transcripts is a good surrogate for Ca^{2+} channel composition and expression in atrial and ventricular muscle of the zebrafish heart. Overall, the present findings show that the diversity of Ca^{2+} channels expressed in the zebrafish heart is higher than that in mammalian hearts and T-type channels are more abundant than L-type Ca^{2+} channels.

T-type Ca^{2+} channel transcript expression

To our knowledge, this is the first quantitative analysis of Ca^{2+} channel composition and expression in the fish heart. The main finding of the present study is that, at the transcript level, T-type Ca^{2+} channels with a relative abundance of 55–64% form the biggest Ca^{2+} channel subfamily in the zebrafish heart. This is in striking contrast to the human heart, where L-type Ca^{2+} channels make up 96–98% of the Ca^{2+} channel transcripts in both atria and ventricles, while T-type Ca^{2+} channels represent only 2–4% of the transcripts (Gaborit et al., 2007). The predominance of T-type Ca^{2+} channels is probably not common among fish hearts in the light of the Ca^{2+} current recordings. I_{CaL} is the main Ca^{2+} current in atrial and ventricular myocytes of many fish species including crucian carp (*Carassius carassius*), rainbow trout (*Oncorhynchus mykiss*), burbot (*Lota lota*) and bluefin tuna (*Thunnus orientalis*) (Vornanen, 1997, 1998; Hove-Madsen and Tort, 1998; Shiels et al., 2006; Shiels et al., 2015). It remains to be shown whether the strong expression of T-type Ca^{2+} channels in ventricles is typical for *Danio*

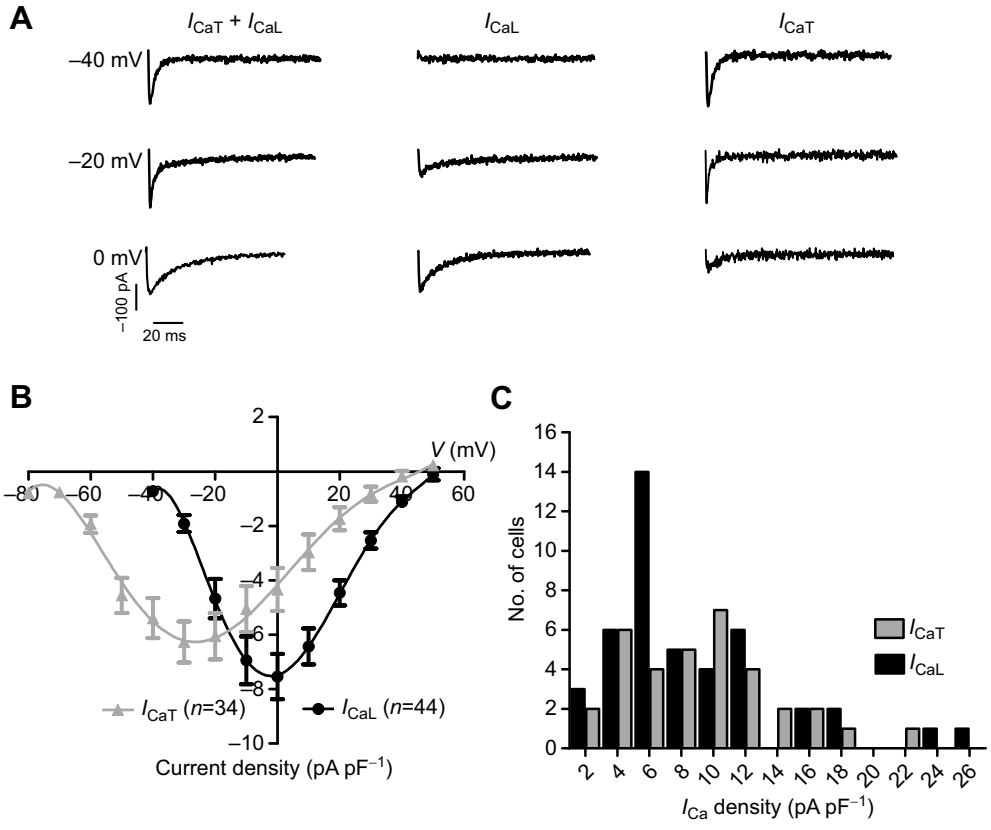

Fig. 3. T-type Ca^{2+} current of zebrafish ventricular myocytes in comparison to L-type Ca^{2+} current. (A) Representative recordings of the voltage dependence of the total cardiac Ca^{2+} current (left) elicited from a holding potential (V_h) of –90 mV, the calcium current through L-type Ca^{2+} channels (I_{CaL}) elicited from a V_h of –50 mV (middle) and the calcium current through T-type Ca^{2+} channels (I_{CaT}) (right) obtained as the difference between the first two currents. (B) Current–voltage dependence of I_{CaT} and I_{CaL} in zebrafish ventricular myocytes. The results are means±s.e.m. of 34 and 44 myocytes for I_{CaT} and I_{CaL}, respectively. (C) Current density histograms of ventricular I_{CaT} and I_{CaL}.

Journal of Experimental Biology (2018) 221, jeb179226. doi:10.1242/jeb.179226

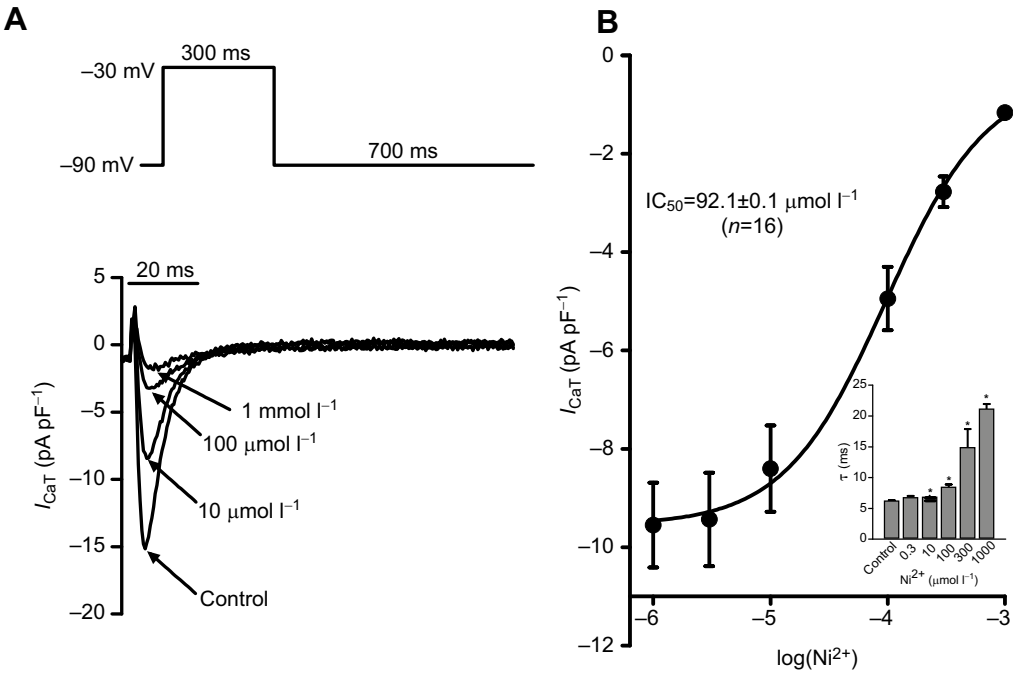

Fig. 4. Concentration-dependent inhibition of zebrafish ventricular I_{CaT} by Ni^{2+}. (A) Representative patch-clamp recordings showing inhibition of I_{CaT} by 10, 100 and 1000 µmol l^{-1} Ni^{2+}. (B) The mean concentration–response curve of Ni^{2+} (mol l^{-1}) inhibition of I_{CaT}. The inset bar graph indicates the concentration-dependent slowing of I_{CaT} inactivation by Ni^{2+}. The results in B are mean values (±s.e.m.) from 6–8 myocytes. An asterisk indicates a statistically significant difference between means in the absence and presence of Ni^{2+} (P<0.05, one-way ANOVA followed by Tukey's *post hoc* test).

species in general (a phylogenetic trait) or is an adaptation of tropical fishes to high environmental temperatures.

In zebrafish heart, five isoforms of T-type Ca^{2+} channels are expressed, while in the human heart only two gene products (*α1H*, *α1G*) are present (Gaborit et al., 2007). Different from mammalian genomes, in the zebrafish genome two paralogues exist for *α1H* and *α1I*, and both gene products are expressed to some extent in the heart. Interestingly, the main T-type Ca^{2+} channel isoform of the zebrafish ventricle is Ca$_v$3.1 (*α1G*). In the right ventricle and Purkinje fibres of the human heart, T-type Ca^{2+} channel transcripts are weakly expressed, and Ca$_v$3.2 (*α1H*) is the predominant isoform in both tissues (Gaborit et al., 2007). In the human right atrium, Ca$_v$3.1 (*α1G*) is the main T-type Ca^{2+} channel isoform, comprising 73.6% of T-type Ca^{2+} channel transcripts and 3.0% of all Ca^{2+} channel transcripts (Gaborit et al., 2007).

The density of I_{CaT} is significantly higher in the ventricles of fetal and neonatal mammals than in the ventricles of adult mammals (Perez-Reyes, 2003; Ono and Iijima, 2010). The developmental decrease in I_{CaT} density of the rat ventricle is associated with a significant shift in isoform composition from predominantly α1G channels to α1H channels (Ferron et al., 2002). mRNA expression of T-type Ca^{2+} channel α1 subunits (*α1G*, *α1H*) in the diseased

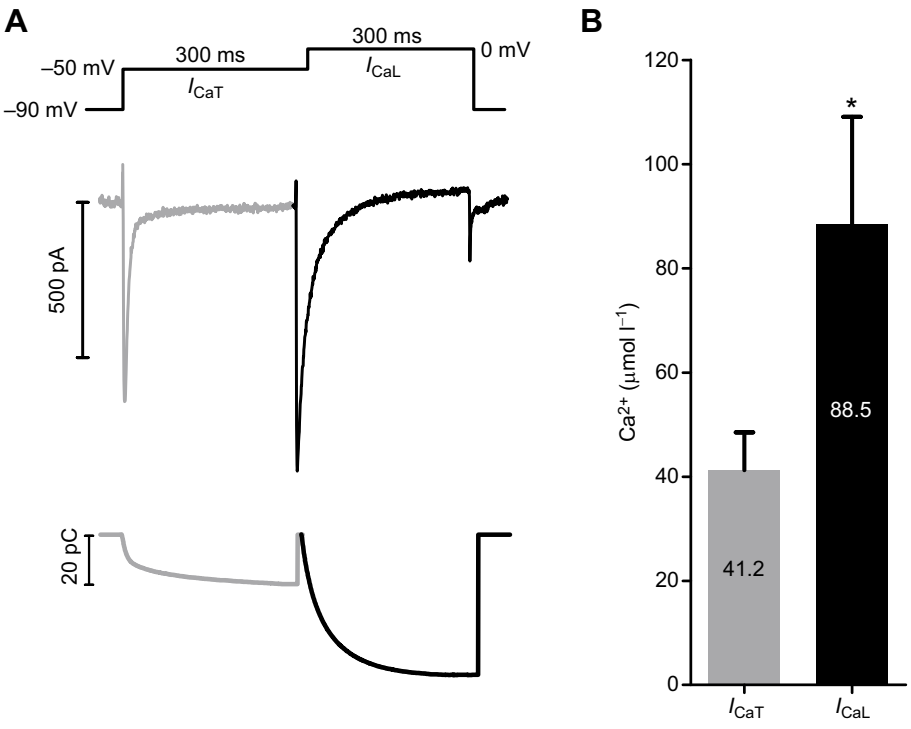

Fig. 5. Sarcolemmal Ca^{2+} influx by T-type Ca^{2+} current: comparison with L-type Ca^{2+} current. (A) Representative recordings of I_{CaT} at –50 mV and I_{CaL} at 0 mV (top trace) and the respective charge integrals (bottom trace). The voltage protocol is shown at the top. (B) Sarcolemmal Ca^{2+} influx by I_{CaT} and I_{CaL} in zebrafish ventricular myocytes. The results are means±s.e.m. from 34 and 44 myocytes for I_{CaT} and I_{CaL}, respectively. An asterisk indicates a statistically significant difference between mean values for I_{CaL} and I_{CaT} (P<0.05, Mann–Whitney U non-parametric test).

Journal of Experimental Biology (2018) 221, jeb179226. doi:10.1242/jeb.179226

(cardiac hypertrophy and failure) mammalian heart is significantly higher than that in healthy controls (Perez-Reyes, 2003; Ono and Iijima, 2010) (see 'Pathophysiology of T-type Ca^{2+} channels', below).

Taken together, the diversity of isoform composition of T-type Ca^{2+} channels is wider in zebrafish ventricle than in human (mammalian) ventricles and the major isoform is $Ca_v3.1$ (encoded by *α1G*) instead of the human $Ca_v3.2$ (encoded by *α1H*). With respect to expression of T-type Ca^{2+} channels, the zebrafish ventricle more closely resembles perinatal and diseased mammalian ventricles than healthy adult mammalian ventricles. Overall, isoform composition of T-type Ca^{2+} channels in zebrafish ventricle is more diverse and relative transcript abundance is markedly higher than in adult human ventricles.

L-type Ca^{2+} channel transcript expression

Instead of the four mammalian L-type Ca^{2+} channel genes, *α1C*, *α1D*, *α1F* and *α1S*, seven isoforms are known for the zebrafish, because *α1D*, *α1F* and *α1S* genes are duplicated. All seven L-type Ca^{2+} channel genes are expressed to some extent in the zebrafish heart. Similar to the human heart (Gaborit et al., 2007), *α1C* (encoding $Ca_v1.2$) is the most expressed L-type Ca^{2+} channel isoform gene in zebrafish atrium and ventricle, and it is almost equally expressed in the two cardiac chambers. Another L-type Ca^{2+} channel expressed in the human heart is $Ca_v1.3$ (*α1D*), but the expression level is quite low, representing 0.04% and 1.13% of all Ca_v1 transcripts in ventricular and atrial myocardia, respectively (Gaborit et al., 2007) (Table 2). In the zebrafish heart, both $Ca_v1.3$ (*α1D*) isoforms are very weakly expressed, whereas $Ca_v1.1$ (*α1Sa*) shows the second highest expression level among the L-type channels in both atrium and ventricle (Fig. 2). Collectively, the relative expression of L-type Ca^{2+} channel transcripts is much lower (41.1% versus 98.4%), and L-type Ca^{2+} channel composition is more diverse in zebrafish than in human heart.

Density of I_{CaT} versus I_{CaL}

Ventricular myocytes of the zebrafish heart have a large I_{CaT}. The peak current density of I_{CaT} is 83.1% of the respective value of I_{CaL}. The slightly smaller density of I_{CaT} in comparison to I_{CaL} is probably due to the lower single channel conductance of the T-type Ca^{2+} channels (Nilius et al., 1985). It should also be noted that the variability of current densities between cells is large for both I_{CaT} and I_{CaL}. Our findings are similar to those of Nemtsas et al. (2010), although our values for I_{CaT} are slightly higher and those for I_{CaL} slightly smaller than theirs. Notably, I_{CaT} has not been found in human atrial and ventricular myocytes, which accords with the minimal expression of the T-type Ca^{2+} channels in the human heart (Beuckelmann et al., 1991; Ouadid et al., 1991; Leuranguer et al., 2001). In contrast, a large cardiac I_{CaT} has previously been documented for a few endothermic and ectothermic vertebrates. A relatively large I_{CaT} exists in ventricular myocytes of finch (5.9 pA pF^{-1}; 56% of I_{CaL}; Bogdanov et al., 1995) and shark (*S. acanthias*; −9.8 pA pF^{-1}; 92.4% of I_{CaL}; Maylie and Morad, 1995), and atrial myocytes of the Siberian sturgeon (*A. baerii*; 3.52 pA pF^{-1}; 242% of I_{CaL}) (Haworth et al., 2014). The peak density of I_{CaT} in zebrafish ventricular myocytes is 2–6 times higher than the reported I_{CaT} density in atrial and nodal tissues of other vertebrate species (for references, see Maylie and Morad, 1995). The presence of a large I_{CaT} in zebrafish ventricular myocytes is one of the most prominent differences in ion current composition between zebrafish and human hearts. I_{CaT} density is significantly higher in the neonatal than in the adult mammalian heart. For example, in the rat ventricle, the density of I_{CaT} decreases from about 3 pA pF^{-1} at the fetal stage F16 to practical absence of the current in the adult ventricle (Ferron et al., 2002).

Ni^{2+} block of T-type Ca^{2+} channels

Ni^{2+} blocks different T-type Ca^{2+} channels with different affinities, and Ni^{2+} sensitivity of the channels is dependent on the cellular environment (Lee et al., 1999). When Ca^{2+} channels were expressed in *Xenopus* oocytes, IC_{50} values were 167, 5.7 and 87 μmol l^{-1} Ni^{2+} for α1G (rat), α1H (human) and α1I (rat), respectively. In HEK-293 cells, the respective IC_{50} values were markedly higher (250, 12 and 216 μmol l^{-1}), even though the relative sensitivity order remained the same. Furthermore, the Ni^{2+} block of α1G and α1I channels (but not of α1H) is voltage dependent, e.g. IC_{50} value of α1G is 200 μmol l^{-1} at 0 mV and only 70 μmol l^{-1} at −40 mV (Lee et al., 1999). In the present study, Ni^{2+} inhibition of I_{CaT} was determined at −30 mV. The IC_{50} value of the zebrafish ventricular I_{CaT} was 92.1 μmol l^{-1}, which is consistent with the T-type Ca^{2+} channel composition dominated by α1G (70 μmol l^{-1} at −40 mV) (Lee et al., 1999). Others have reported a slightly higher IC_{50} value (124 μmol l^{-1}) for the zebrafish ventricular I_{CaT} at −40 mV (Nemtsas et al., 2010). The high Ni^{2+} sensitivity of α1H channels is related to a unique histidine residue at position 191 in the S3–S4 loop of domain I (Kang et al., 2007). Sequence analysis of zebrafish T-type Ca^{2+} channel genes indicates that channels encoded by *α1H* and *α1G*, but not *α1I*, share histidine-191 with the mammalian α1H.

Ca^{2+} influx via I_{CaT} and its physiological significance

In canine Purkinje myocytes, guinea-pig ventricular myocytes and mouse ventricular myocytes overexpressing α1G T-type Ca^{2+} channels, Ca^{2+} admitted through T-type Ca^{2+} channels is capable of activating contraction via CICR from the SR (Sipido et al., 1998; Zhou and January, 1998; Jaleel et al., 2008). However, contractions initiated by Ca^{2+} entry through T-type Ca^{2+} channels are characterized by a long delay to the onset of shortening, slow rates of shortening and relaxation, low peak shortening, and long time-to-peak shortening (Zhou and January, 1998; Sipido et al., 1998; Jaleel et al., 2008). These findings show that Ca^{2+} entry through I_{CaT} is less effective than that through I_{CaL} in triggering CICR. T-type Ca^{2+} channels are primarily located in the peripheral sarcolemma and therefore are more distant from the Ca^{2+} release channels of the SR than L-type Ca^{2+} channels of the T-tubule membrane (Jaleel et al., 2008).

The contraction of zebrafish ventricle is strongly dependent on sarcolemmal Ca^{2+} influx, while CICR from the SR makes only a small contribution (about 15%) to the Ca^{2+} transient (Zhang et al., 2011; Bovo et al., 2013). In keeping with this, the combined sarcolemmal Ca^{2+} influx via I_{CaL} and I_{CaT} in zebrafish ventricular myocytes (129 μmol l^{-1} at 28°C) is markedly large, bigger than that in other fish species like rainbow trout (32.1–45.8 μmol l^{-1} at 21°C) and crucian carp (14.7–42.9 μmol l^{-1} at 19–23°C) (Vornanen, 1997, 1998; Hove-Madsen and Tort, 1998). Moreover, in zebrafish ventricular myocytes, a significant portion of this Ca^{2+} influx is mediated by I_{CaT}. Indeed, T-type Ca^{2+} channels could be important for E–C coupling of cardiac myocytes in zebrafish and other tropical ectotherms, which rely strongly on sarcolemmal Ca^{2+} influx for cardiac contraction. Because of its low voltage threshold (about −70 mV), I_{CaT} starts to contribute to the intracellular Ca^{2+} transient earlier in the AP than I_{CaL}, which has a more depolarized threshold (about −40 mV). This is expected to reduce the delay between membrane depolarization and the onset of the intracellular Ca^{2+} transient, and make the Ca^{2+} transient fast rising. Fast Ca^{2+}

transients might be adaptive for the tropical *Danio* species, which have high heart rates at temperatures close to their upper thermal tolerance limit (Sidhu et al., 2014). For example, in *D. rerio* at 36°C, the heart beats about 300 times per minute and ventricular AP lasts (AP duration at 50% repolarization) only 66 ms (Vornanen and Hassinen, 2016). At high temperatures, I_{CaT} and fast Ca^{2+} transients may be needed to cope with the requirements of short cycle lengths and AP durations. The role of I_{CaT} in cardiac E–C coupling of zebrafish and other tropical fish species will be an interesting future topic.

Pathophysiology of T-type Ca^{2+} channels

T-type Ca^{2+} channels and I_{CaT} are present in ventricular myocytes of perinatal mammalian (e.g. rat and mouse) heart, but during early postnatal development they gradually disappear (Ferron et al., 2002; Yasui et al., 2005). T-type Ca^{2+} channels and I_{CaT} reappear in ventricular myocytes of hypertrophied mammalian heart under different pathological stresses (Nuss and Houser, 1993; Martinez et al., 1999; Takebayashi et al., 2006), suggesting that they are somehow involved in the pathogenesis of hypertrophy. Indeed, studies on transgenic mouse models suggest that $Ca_v3.2$ (*α1H*) channels might be pro-hypertrophic and $Ca_v3.1$ (*α1G*) channels anti-hypertrophic (Chiang et al., 2009; Nakayama et al., 2009). It should be noted, however, that in ventricular myocytes of perinatal mammals and adult zebrafish, I_{CaT} is a normal physiological component of the sarcolemmal ion current complex. In the ventricle of zebrafish, I_{CaT} is largely generated by $Ca_v3.1$ (*α1G*) channels, while in the ventricles of embryonic and neonatal mouse, $Ca_v3.2$ (*α1H*) channels predominate (Ferron et al., 2002; Yasui et al., 2005).

Hypertrophic heart is prone to cardiac arrhythmias, but the role of the re-expressed T-type Ca^{2+} channels in arrhythmogenesis of mammalian heart is not yet resolved (Kinoshita et al., 2009). Steady-state activation and inactivation curves of mammalian I_{CaT} overlap, which shows that a small portion of the channels do not inactivate (Vassort et al., 2006). The non-inactivating T-type Ca^{2+} channels could be involved in arrhythmogenesis by inducing early and delayed after-depolarizations and associated arrhythmias (Kinoshita et al., 2009). The role of I_{CaT} is, however, difficult to discern as many other ion currents are changed in parallel with I_{CaT} (Kinoshita et al., 2009). It should be noted, however, that delayed after-depolarizations are induced by spontaneous Ca^{2+} release from the SR and SR leak may also be involved in triggering early after-depolarizations (Choi et al., 2002). In fish ventricular myocytes, Ca^{2+} release channels of the SR have low affinity to Ca^{2+} and therefore spontaneous Ca^{2+} releases are rare (Shiels and White, 2005; Vornanen, 2006; Bovo et al., 2013). The minor role of CICR in fish cardiac E–C coupling is suggested to make fish hearts less susceptible to early and delayed after-depolarizations and therefore triggered arrhythmias (Vornanen, 2017).

Conclusions and future perspectives

Zebrafish ventricular myocytes have a large I_{CaT}, which contributes a distinct depolarizing current and relatively large sarcolemmal Ca^{2+} influx. This is a prominent difference to human ventricles, where I_{CaL} is apparently the sole Ca^{2+} current type (Beuckelmann et al., 1991; Leuranguer et al., 2001). These differences are due to the dominance of T-type Ca^{2+} channels in the zebrafish heart (present study) and L-type Ca^{2+} channels in the human heart (Gaborit et al., 2007). As the zebrafish is a popular model for drug screening and human cardiac toxicology (Barros et al., 2008; Chakraborty et al., 2009; Peterson and MacRae, 2012), these species-specific differences in electrical excitation and E–C coupling warrant some care when adapting results from zebrafish studies to human heart. Because of the significant differences in Ca^{2+} and K^+ currents/channels between zebrafish and human ventricles (Hassinen et al., 2015; Vornanen and Hassinen, 2016), the zebrafish is probably not an optimal model for screening of cardiovascular drugs. Interspecies differences in cardiac ion currents are so marked (even among mammals) that non-human cells and tissues are considered unsatisfying for preclinical drug screening and safety pharmacology. According to the novel CiPA (Comprehensive *in vitro* Proarrhythmia Assay) initiative of preclinical drug screening, only human cardiac ion channels, human stem cell-induced cardiomyocytes and *in silico* models of human cardiac AP are considered acceptable for drug screening and safety pharmacology (Gintant et al., 2016). CIPA is based on analysis of drug effects on multiple (7) human cardiac ion channels (Colatsky et al., 2016; Vicente et al., 2016), and I_{CaT} is not among those channels. If zebrafish are used for preclinical drug screening and safety pharmacology, the potential impact of the large I_{CaT} on drug responses and arrhythmia propensity should be carefully examined.

Although zebrafish may not be an optimal general model for human cardiac safety pharmacology and screening of cardiac drugs, they may be useful in solving more specific problems of ion channel function in cardiac excitation and E–C coupling. Owing to the large ventricular I_{CaT}, zebrafish could be a useful model species when the role of I_{CaT} in cardiac E–C coupling and as a putative target for cardiovascular drugs is examined. With their large I_{CaT}, lower dependence on CICR from the SR and absence of T-tubules, zebrafish ventricular myocytes more closely resemble perinatal ventricular myocytes than adult ventricular myocytes of the human heart. Considering that there is a paucity of information regarding the cardiac safety pharmacology of human neonates and premature infants (Pesco-Koplowitz et al., 2018), zebrafish could be a useful model for this population.

Acknowledgements

Prof. Pertti Panula (University of Helsinki) is acknowledged for donating the zebrafish for the establishment of our own zebrafish population in Joensuu. Anita Kervinen kindly prepared the solutions for electrophysiological experiments.

Competing interests

The authors declare no competing or financial interests.

Author contributions

Methodology: J.H., M.H., S.N.D., M.V.; Investigation: J.H., S.N.D.; Resources: M.V.; Writing - original draft: J.H., M.H., S.N.D., M.V.; Visualization: J.H., M.H., M.V.; Supervision: M.V.; Project administration: M.V.; Funding acquisition: M.V.

Funding

This work was supported by Jane ja Aatos Erkon Säätiö (project no. 64579 to M.V.).

References

Abd Allah, E. S., Aslanidi, O. V., Tellez, J. O., Yanni, J., Billeter, R., Zhang, H., Dobrzynski, H. and Boyett, M. R. (2012). Postnatal development of transmural gradients in expression of ion channels and Ca^{2+}-handling proteins in the ventricle. *J. Mol. Cell. Cardiol.* **53**, 145-155.

Bakkers, J. (2011). Zebrafish as a model to study cardiac development and human cardiac disease. *Cardiovasc. Res.* **91**, 279-288.

Balke, C. W., Rose, W. C., Marban, E. and Wier, W. G. (1992). Macroscopic and unitary properties of physiological ion flux through T-type Ca^{2+} channels in guinea-pig heart cells. *J. Physiol.* **456**, 247-265.

Barros, T. P., Alderton, W. K., Reynolds, H. M., Roach, A. G. and Berghmans, S. (2008). Zebrafish: an emerging technology for in vivo pharmacological assessment to identify potential safety liabilities in early drug discovery. *Br. J. Pharmacol.* **154**, 1400-1413.

Belardetti, F. and Zamponi, G. W. (2012). Calcium channels as therapeutic targets. *Wiley Interdiscip. Rev. Dev. Biol.* **1**, 433-451.

Bers, D. M. (2002). Cardiac excitation-contraction coupling. *Nature* **415**, 198-205.

Beuckelmann, D. J., Näbauer, M. and Erdmann, E. (1991). Characteristics of calcium-current in isolated human ventricular myocytes from patients with terminal heart failure. *J. Mol. Cell. Cardiol.* **23**, 929-937.
Bogdanov, K. Y., Ziman, B. D., Spurgeon, H. A. and Lakatta, E. G. (1995). L-type and T-type calcium currents differ in finch and rat ventricular cardiomyocytes. *J. Mol. Cell. Cardiol.* **27**, 2581-2593.
Bovo, E., Dvornikov, A. V., Mazurek, S. R., de Tombe, P. P. and Zima, A. V. (2013). Mechanisms of Ca^{2+} handling in zebrafish ventricular myocytes. *Pflügers Arch.* **465**, 1775-1784.
Brette, F., Luxan, G., Cros, C., Dixey, H., Wilson, C. and Shiels, H. A. (2008). Characterization of isolated ventricular myocytes from adult zebrafish (*Danio rerio*). *Biochem. Biophys. Res. Commun.* **374**, 143-146.
Catterall, W. A., Perez-Reyes, E., Snutch, T. P. and Striessnig, J. (2005). International Union of Pharmacology. XLVIII. Nomenclature and structure-function relationships of voltage-gated calcium channels. *Pharmacol. Rev.* **57**, 411-425.
Chakraborty, C., Hsu, C. H., Wen, Z. H., Lin, C. S. and Agoramoorthy, G. (2009). Zebrafish: a complete animal model for in vivo drug discovery and development. *Curr. Drug Metab.* **10**, 116-124.
Chandler, N. J., Greener, I. D., Tellez, J. O., Inada, S., Musa, H., Molenaar, P., DiFrancesco, D., Baruscotti, M., Longhi, R., Anderson, R. H. et al. (2009). Molecular architecture of the human sinus node: insights into the function of the cardiac pacemaker. *Circulation* **119**, 1562-1575.
Chiang, C.-S., Huang, C.-H., Chieng, H., Chang, Y.-T., Chang, D., Chen, J.-J., Chen, Y.-C., Chen, Y.-H., Shin, H.-S., Campbell, K. P. et al. (2009). The $Ca_v3.2$ T-type Ca^{2+} channel is required for pressure overload-induced cardiac hypertrophy in mice. *Circ. Res.* **104**, 522-530.
Choi, B.-R., Burton, F. and Salama, G. (2002). Cytosolic Ca^{2+} triggers early afterdepolarizations and Torsade de Pointes in rabbit hearts with type 2 long QT syndrome. *J. Physiol.* **543**, 615-631.
Colatsky, T., Fermini, B., Gintant, G., Pierson, J. B., Sager, P., Sekino, Y., Strauss, D. G. and Stockbridge, N. (2016). The comprehensive in vitro proarrhythmia assay (CiPA) initiative - Update on progress. *J. Pharmacol. Toxicol. Methods* **81**, 15-20.
Ertel, E. A., Campbell, K. P., Harpold, M. M., Hofmann, F., Mori, Y., Perez-Reyes, E., Schwartz, A., Snutch, T. P., Tanabe, T. and Birnbaumer, L. (2000). Nomenclature of voltage-gated calcium channels. *Neuron* **25**, 533-535.
Fabiato, A. (1983). Calcium-induced release of calcium from the cardiac sarcoplasmic reticulum. *Am. J. Physiol.* **245**, C1-C14.
Fabiato, A. and Fabiato, F. (1978). Calcium-induced release of calcium from the sarcoplasmic reticulum of skinned cells from adult human, dog, cat, rabbit, rat and frog hearts and from fetal and new-born rat ventricles. *Ann. NY Acad. Sci.* **307**, 491-522.
Ferron, L., Capuano, V., Deroubaix, E., Coulombe, A. and Renaud, J.-F. (2002). Functional and molecular characterization of a T-type Ca^{2+} channel during fetal and postnatal rat heart development. *J. Mol. Cell. Cardiol.* **34**, 533-546.
Gaborit, N., Le Bouter, S., Szuts, V., Varro, A., Escande, D., Nattel, S. and Demolombe, S. (2007). Regional and tissue specific transcript signatures of ion channel genes in the non-diseased human heart. *J. Physiol.* **582**, 675-693.
Galli, G. L. J., Lipnick, M. S., Shiels, H. A. and Block, B. A. (2011). Temperature effects on Ca^{2+} cycling in scombrid cardiomyocytes: a phylogenetic comparison. *J. Exp. Biol.* **214**, 1068-1076.
Gintant, G., Sager, P. T. and Stockbridge, N. (2016). Evolution of strategies to improve preclinical cardiac safety testing. *Nat. Rev. Drug Discov.* **15**, 457.
Hagiwara, N., Irisawa, H. and Kameyama, M. (1988). Contribution of two types of calcium currents to the pacemaker potentials of rabbit sino-atrial node cells. *J. Physiol.* **395**, 233-253.
Hassinen, M., Haverinen, J., Hardy, M. E., Shiels, H. A. and Vornanen, M. (2015). Inward rectifier potassium current (I_{K1}) and Kir2 composition of the zebrafish (*Danio rerio*) heart. *Pflüg. Arch. Eur. J. Physiol.* **467**, 2437-2446.
Haverinen, J., Egginton, S. and Vornanen, M. (2014). Electrical excitation of the heart in a basal vertebrate, the European river lamprey (*Lampetra fluviatilis*). *Physiol. Biochem. Zool.* **87**, 817-828.
Haworth, T. E., Haverinen, J., Shiels, H. A. and Vornanen, M. (2014). Electrical excitability of the heart in a Chondrostei fish, the Siberian sturgeon (*Acipenser baerii*). *Am. J. Physiol.* **307**, R1157-R1166.
Hofmann, F., Flockerzi, V., Kahl, S. and Wegener, J. W. (2014). L-type CaV1.2 calcium channels: from in vitro findings to in vivo function. *Physiol. Rev.* **94**, 303-326.
Hove-Madsen, L. and Tort, L. (1998). L-type Ca^{2+} current and excitation-contraction coupling in single atrial myocytes from rainbow trout. *Am. J. Physiol.* **275**, R2061-R2069.
Irisawa, H., Brown, H. F. and Giles, W. (1993). Cardiac pacemaking in the sinoatrial node. *Physiol. Rev.* **73**, 197-227.
Jaleel, N., Nakayama, H., Chen, X., Kubo, H., MacDonnell, S., Zhang, H., Berretta, R., Robbins, J., Cribbs, L. L., Molkentin, J. D. et al. (2008). Ca^{2+} influx through T- and L-type Ca^{2+} channels have different effects on myocyte contractility and induce unique cardiac phenotypes. *Circ. Res.* **103**, 1109-1119.
Jegla, T. J., Zmasek, C. M., Batalov, S. and Nayak, S. K. (2009). Evolution of the human ion channel set. *Comb. Chem. High Throughput Screen.* **12**, 2-23.
Kang, H.-W., Moon, H.-J., Joo, S.-H. and Lee, J.-H. (2007). Histidine residues in the IS3–IS4 loop are critical for nickel-sensitive inhibition of the Cav2.3 calcium channel. *FEBS Lett.* **581**, 5774-5780.
Kinoshita, H., Kuwahara, K., Takano, M., Arai, Y., Kuwabara, Y., Yasuno, S., Nakagawa, Y., Nakanishi, M., Harada, M., Fujiwara, M. et al. (2009). T-type Ca^{2+} channel blockade prevents sudden death in mice with heart failure. *Circulation* **120**, 743-752.
Kitchens, S. A., Burch, J. and Creazzo, T. L. (2003). T-type Ca^{2+} current contribution to Ca^{2+}-induced Ca^{2+} release in developing myocardium. *J. Mol. Cell. Cardiol.* **35**, 515-523.
Lee, J.-H., Gomora, J. C., Cribbs, L. L. and Perez-Reyes, E. (1999). Nickel block of three cloned T-Type calcium channels: low concentrations selectively block α1H. *Biophys. J.* **77**, 3034-3042.
Leuranguer, V., Mangoni, M. E., Nargeot, J. and Richard, S. (2001). Inhibition of T-Type and L-Type calcium channels by mibefradil: physiologic and pharmacologic bases of cardiovascular effects. *J. Cardiovasc. Pharmacol.* **37**, 649-661.
MacRae, C. A. and Peterson, R. T. (2015). Zebrafish as tools for drug discovery. *Nature Reviews Drug Discovery* **14**, 721-731.
Marionneau, C., Couette, B., Liu, J., Li, H., Mangoni, M. E., Nargeot, J., Lei, M., Escande, D. and Demolombe, S. (2005). Specific pattern of ionic channel gene expression associated with pacemaker activity in the mouse heart. *J. Physiol.* **562**, 223-234.
Martinez, M. L., Heredia, M. P. and Delgado, C. (1999). Expression of T-type Ca^{2+} channels in ventricular cells from hypertrophied rat hearts. *J. Mol. Cell. Cardiol.* **31**, 1617-1625.
Maylie, J. G. and Morad, M. (1995). Evaluation of T-type and L-type Ca^{2+} currents in shark ventricular myocytes. *Am. J. Physiol.* **269**, H1695-H1703.
McDonald, T. F., Pelzer, S., Trautwein, W. and Pelzer, D. J. (1994). Regulation and modulation of calcium channels in cardiac, skeletal, and smooth muscle cells. *Physiol. Rev.* **74**, 365-507.
Mesirca, P., Torrente, A. G. and Mangoni, M. E. (2015). Functional role of voltage gated Ca^{2+} channels in heart automaticity. *Front. Physiol.* **6**, 19.
Mitra, R. and Morad, M. (1986). Two types of calcium channels in guinea pig ventricular myocytes. *Proc. Natl. Acad. Sci. USA* **83**, 5340-5344.
Morad, M., Goldman, Y. E. and Trentham, D. R. (1981). Rapid photochemical inactivation of Ca^{2+}-antagonits shows that Ca^{2+} entry directly activates contraction in frog heart. *Nature* **304**, 635-638.
Nakayama, H., Bodi, I., Correll, R. N., Chen, X., Lorenz, J., Houser, S. R., Robbins, J., Schwartz, A. and Molkentin, J. D. (2009). Alpha1G-dependent T-type Ca^{2+} current antagonizes cardiac hypertrophy through a NOS3-dependent mechanism in mice. *J. Clin. Invest.* **119**, 3787-3796.
Nemtsas, P., Wettwer, E., Christ, T., Weidinger, G. and Ravens, U. (2010). Adult zebrafish heart as a model for human heart? An electrophysiological study. *J. Mol. Cell. Cardiol.* **48**, 161-171.
Nilius, B., Hess, P., Lansman, J. B. and Tsien, R. W. (1985). A novel type of cardiac calcium channel in ventricular cells. *Nature* **316**, 443-446.
Nuss, H. B. and Houser, S. R. (1993). T-type Ca^{2+} current is expressed in hypertrophied adult feline left ventricular myocytes. *Circ. Res.* **73**, 777-782.
Ono, K. and Iijima, T. (2010). Cardiac T-type Ca^{2+} channels in the heart. *J. Mol. Cell. Cardiol.* **48**, 65-70.
Ouadid, H., Séguin, J., Richard, S., Chaptal, P. A. and Nargeot, J. (1991). Properties and modulation of Ca channels in adult human atrial cells. *J. Mol. Cell. Cardiol.* **23**, 41-54.
Perez-Reyes, E. (2003). Molecular physiology of low-voltage-activated t-type calcium channels. *Physiol. Rev.* **83**, 117-161.
Pesco-Koplowitz, L., Gintant, G., Ward, R., Heon, D., Saulnier, M. and Heilbraun, J. (2018). Drug-induced cardiac abnormalities in premature infants and neonates. *Am. Heart J.* **195**, 14-38.
Peterson, R. T. and MacRae, C. A. (2012). Systematic approaches to toxicology in the zebrafish. *Annu. Rev. Pharmacol. Toxicol.* **52**, 433-453.
Rosati, B. and McKinnon, D. (2004). Regulation of ion channel expression. *Circ. res.* **94**, 874-883.
Rottbauer, W., Baker, K., Wo, Z. G., Mohideen, M.-A. P. K., Cantiello, H. F. and Fishman, M. C. (2001). Growth and function of the embryonic heart depend upon the cardiac-specific L-Type calcium channel α1 subunit. *Dev. Cell* **1**, 265-275.
Shiels, H. A. and White, E. (2005). Temporal and spatial properties of cellular Ca^{2+} flux in trout ventricular myocytes. *Am. J. Physiol.* **288**, R1756-R1766.
Shiels, H. A., Paajanen, V. and Vornanen, M. (2006). Sarcolemmal ion currents and sarcoplasmic reticulum Ca^{2+} content in ventricular myocytes from the cold stenothermic fish, the burbot (*Lota lota*). *J. Exp. Biol.* **209**, 3091-3100.
Shiels, H. A., Galli, G. L. J. and Block, B. A. (2015). Cardiac function in an endothermic fish: cellular mechanisms for overcoming acute thermal challenges during diving. *Proc. R. Soc. Lond. B* **282**, 20141989.
Sidhu, R., Anttila, K. and Farrell, A. P. (2014). Upper thermal tolerance of closely related *Danio* species. *J. Fish Biol.* **84**, 982-995.
Sipido, K. R., Carmeliet, E. and Van de Werf, F. (1998). T-type Ca^{2+} current as trigger for Ca^{2+} release from the sarcoplasmic reticulum in guinea-pig ventricular myocytes. *J. Physiol.* **508.2**, 439-451.

Takebayashi, S., Li, Y., Kaku, T., Inagaki, S., Hashimoto, Y., Kimura, K., Miyamoto, S. H. T. and Ono, K. (2006). Remodeling excitation–contraction coupling of hypertrophied ventricular myocytes is dependent on T-type calcium channels expression. *Biochem. Biophys. Res. Commun.* **345**, 766-773.

Vassort, G., Talavera, K. and Alvarez, J. L. (2006). Role of T-type Ca^{2+} channels in the heart. *Cell Calcium* **40**, 205-220.

Vicente, J., Stockbridge, N. and Strauss, D. G. (2016). Evolving regulatory paradigm for proarrhythmic risk assessment for new drugs. *J. Electrocardiol.* **49**, 837-842.

Vornanen, M. (1996). Contribution of calcium current to total cellular calcium in postnatally developing rat heart. *Cardiovasc. Res.* **32**, 400-410.

Vornanen, M. (1997). Sarcolemmal Ca influx through L-type Ca channels in ventricular myocytes of a teleost fish. *Am. J. Physiol.* **272**, R1432-R1440.

Vornanen, M. (1998). L-type Ca current in fish cardiac myocytes: effects of thermal acclimation and β-adrenergic stimulation. *J. Exp. Biol.* **201**, 533-547.

Vornanen, M. (2006). Temperature and Ca^{2+} dependence of [^{3}H]ryanodine binding in the burbot (*Lota lota* L.) heart. *Am. J. Physiol.* **290**, R345-R351.

Vornanen, M. (2017). Electrical excitability of the fish heart and its autonomic regulation. In *The Cardiovascular System: Morphology, Control and Function (Fish Physiology)* (ed. K. A. Gamperl, T. E. Gillis, P. A. Farrell and C. J. Brauner), pp. 99-153. Cambridge, MA: Elsevier.

Vornanen, M. and Hassinen, M. (2016). Zebrafish heart as a model for human cardiac electrophysiology. *Channels* **10**, 101-110.

Vornanen, M., Shiels, H. A. and Farrell, A. P. (2002). Plasticity of excitation-contraction coupling in fish cardiac myocytes. *Comp. Biochem. Physiol. A* **132**, 827-846.

Wang, H.-S. and Cohen, I. S. (2003). Calcium channel heterogeneity in canine left ventricular myocytes. *J. Physiol.* **547**, 825-833.

Warren, K. S., Baker, K. and Fishman, M. C. (2001). The slow mo mutation reduces pacemaker current and heart rate in adult zebrafish. *Am. J. Physiol.* **281**, H1711-H1719.

Westerfield, M. (2007). *The Zebrafish Book: A Guide for the Laboratory use of Zebrafish Danio (Brachydanio rerio)*. Eugene, Oregon, USA: University of Oregon Press.

Wong, E., Yu, W.-P., Yap, W. H., Venkatesh, B. and Soong, T. W. (2006). Comparative genomics of the human and Fugu voltage-gated calcium channel α1-subunit gene family reveals greater diversity in Fugu. *Gene* **366**, 117-127.

Yasui, K., Niwa, N., Takemura, H., Opthof, T., Muto, T., Horiba, M., Shimizu, A., Lee, J.-K., Honjo, H. and Kamiya, K. (2005). Pathophysiological significance of T-type Ca^{2+} channels: expression of T-type Ca^{2+} channels in fetal and diseased heart. *J. Pharmacol. Sci.* **99**, 205-210.

Zamponi, G. W., Striessnig, J., Koschak, A. and Dolphin, A. C. (2015). The physiology, pathology, and pharmacology of voltage-gated calcium channels and their future therapeutic potential. *Pharmacol. Rev.* **67**, 821-870.

Zhang, P. C., Llach, A., Sheng, X. Y., Hove-Madsen, L. and Tibbits, G. F. (2011). Calcium handling in zebrafish ventricular myocytes. *Am. J. Physiol.* **300**, R56-R66.

Zhou, Z. and January, C. T. (1998). Both T- and L-type Ca^{2+} channels can contribute to excitation-contraction coupling in cardiac Purkinje cells. *Biophys. J.* **74**, 1830-1839.